Mapping leucocyte populations in mouse lymphoid tissues and blood

Using a 28-color panel on the BD FACSymphony™ system

Features

- Comprehensive immunophenotyping panel for assessing cell composition across different tissues
- Simplified and robust data analysis using the cell-clustering algorithms in FlowJo™ v10 software
- High-resolution identification of over 15 distinct mouse leucocyte subsets

Multiparameter analysis of single cells allows the enumeration and characterization of heterogeneous cell phenotypes in a variety of infectious diseases, blood cancers, immunodeficiencies and other disorders. Recently, significant growth in multiparameter cell analysis has been observed in the field of immuno-oncology, as a way to understand the complexity and systemic nature of the immune response in cancer immunotherapies. Supported by recent advances in reagent development and instrumentation, this approach has enabled increasing dimensionality in single cell data collection and accelerated the discovery and testing of new therapies.

The BD FACSymphony™ cell analyzer used in this experiment allows the simultaneous analysis of up to 28 colors and 30 parameters in a single tube. This instrument can detect a series of very bright BD Horizon Brilliant™ Blue, BD Horizon Brilliant™ Violet and BD Horizon Brilliant™ Ultraviolet dyes, providing flexibility in panel design and better sensitivity for detecting low-expressed antigens.

In this data sheet, we describe a 28-color panel that was designed to identify and characterize various subpopulations of mouse leucocytes that play a role in both innate and adaptive immune responses. The panel was developed so that it could be applied in cell analyses across varying lymphoid tissues and blood.

BD

Some of the markers used in the panel identify the major cell populations, including B cells ($CD45R^+CD19^+$), T cells ($CD3\varepsilon^+CD4^+$ or $CD8\alpha^+$), natural killer cells (NK, $NK1.1^+$) and dendritic cells (DCs, $CD11c^+$) as well as monocytes, macrophages and neutrophils. Other markers allow further differentiation of these populations into subsets, such as naïve and memory T cells. Two of the markers employed in the panel, CD25 and CD192, are known to be upregulated upon cell activation on T cells and monocytes, respectively. CD25 and CD127 can also be used for characterization of regulatory T cells and subsets of B-cell progenitors. In addition to a total of 27 antibodies, the cells were stained with BD Pharmingen™ 7-AAD for exclusion of dead cells from the analyses (Figures 1A and 1B).

Figure 1A

B Cells $CD19^+$

Immature/ Transitional	Marginal Zone	Follicular	B-1a
$B220^+$	$B220^+$	$B220^+$	$B220^{low}$
IgM^{high}	IgM^+	IgD^{high}	$CD43^+$
$CD93^+$	$CD21^{high}$	$CD23^+$	$CD5^+$

T Cells $CD3\varepsilon^+$

CD4 Naïve	CD8 Naïve	Central Memory	Effector Memory
$CD4^+$	$CD8^+$	$CD62L^+$	$CD62L^{low}$
$CD62L^{high}$	$CD62L^{high}$	$CD44^{high}$	$CD44^{high}$

Dendritic Cells $CD11c^+$

Myeloid	Lymphoid	Plasmacytoid
IA/IE^{high}	IA/IE^{high}	IA/IE^{low}
$CD11b^+$	$CD8\alpha^+$	$B220^+$

Monocytes and Macrophages $CD11b^+$

Macrophages	Monocyte Subsets
$Ly6C^{low}$	$Ly6C^{high}$
$F4/80^{high}$	$Ly6C^{low}$

NK Cells $NK1.1^+$

$CD27^{high/low}$
$CD11b^{high/low}$
$NKG2A^{+/-}$

Neutrophils $CD11b^+$

$Ly6C^{low}$
$Ly6G^+$

Figure 1B

Laser	Fluorochrome	Marker
Ultraviolet 355 nm 40 mW	BUV805	CD45R/B220
	BUV737	Ly6C
	BUV661	CD21
	BUV615	CD314/NKG2D
	BUV563	F4/80
	BUV496	IgD
	BUV395	CD8α
Violet 405 nm 100 mW	BV786	IgM
	BV750	CD25
	BV711	CD27
	BV650	CD23
	BV605	CD192
	BV570	CD4
	BV480	IA/IE
	BV421	CD44
Blue 488 nm 100 mW	BB790	NK1.1
	BB755	Ly6G
	7-AAD	live/dead
	BB660	CD127
	BB630	CD11c
	BB515	CD62L
	SSC	
Yellow-Green 561 nm 150 mW	PE-Cy™7	CD43
	PE-Cy™5	NKG2A/C/E
	PE-CF594	CD93
	PE	CD5
Red 628 nm 200 mW	APC-H7	CD19
	APC-R700	CD11b
	APC	CD3ε

Figure 1. 28-color panel for analysis of immune cell composition in different mouse tissues

A. Description of the major leucocyte cell populations based on the expression of cell lineage and cell differentiation surface markers. **B.** BD FACSymphony instrument laser configuration and antibody conjugates used in the 28-color panel.

The tissues were processed and data was acquired in BD FACSDiva™ software and analyzed in FlowJo™ software, as described in Figure 2. After doublet exclusion and gating of live cells, the cells from bone marrow, blood, spleen and lymph nodes were reduced to 10,000 events each and merged into one file, in which t-Distributed Stochastic Neighbor Embedding (t-SNE) was applied (Figure 2A). The clusters created with t-SNE were arbitrarily selected and annotated as indicated by the numbers. Subsequently, the FlowSOM algorithm was applied to the same dataset and generated the colored clusters shown on the t-SNE map (Figure 2B).

FlowSOM and t-SNE formed essentially similar clusters and revealed five main cell islands containing B cells, CD4$^+$ T cells, CD8$^+$ T cells, NK cells and myeloid cells. To study the distribution of those cell populations across the tissues, the individual samples were analyzed in the t-SNE map generated from the merged dataset (Figures 2C and 2D). This approach demonstrated cell compartmentalization, for example, most of the myeloid cells resided in the bone marrow whereas lymphocyte populations were localized mostly in the secondary lymphoid tissues. Conversely, NK cells, as well as a smaller fraction of cells within cluster one, were found mostly in the blood.

The expression of the various markers in the panel could also be visualized in a FlowSOM spanning tree. Representative analysis of the expression of CD11b, NK1.1, CD19 and CD3ε revealed the location of myeloid cells, NK cells, B cells and T cells, respectively, in the spanning tree (Figure 2E). Similarly to the phenotypes observed in the t-SNE map, each cell lineage in the spanning tree occupied a distinct location. This confirms the effectiveness of our 28-color panel in dissecting the major populations of leucocytes.

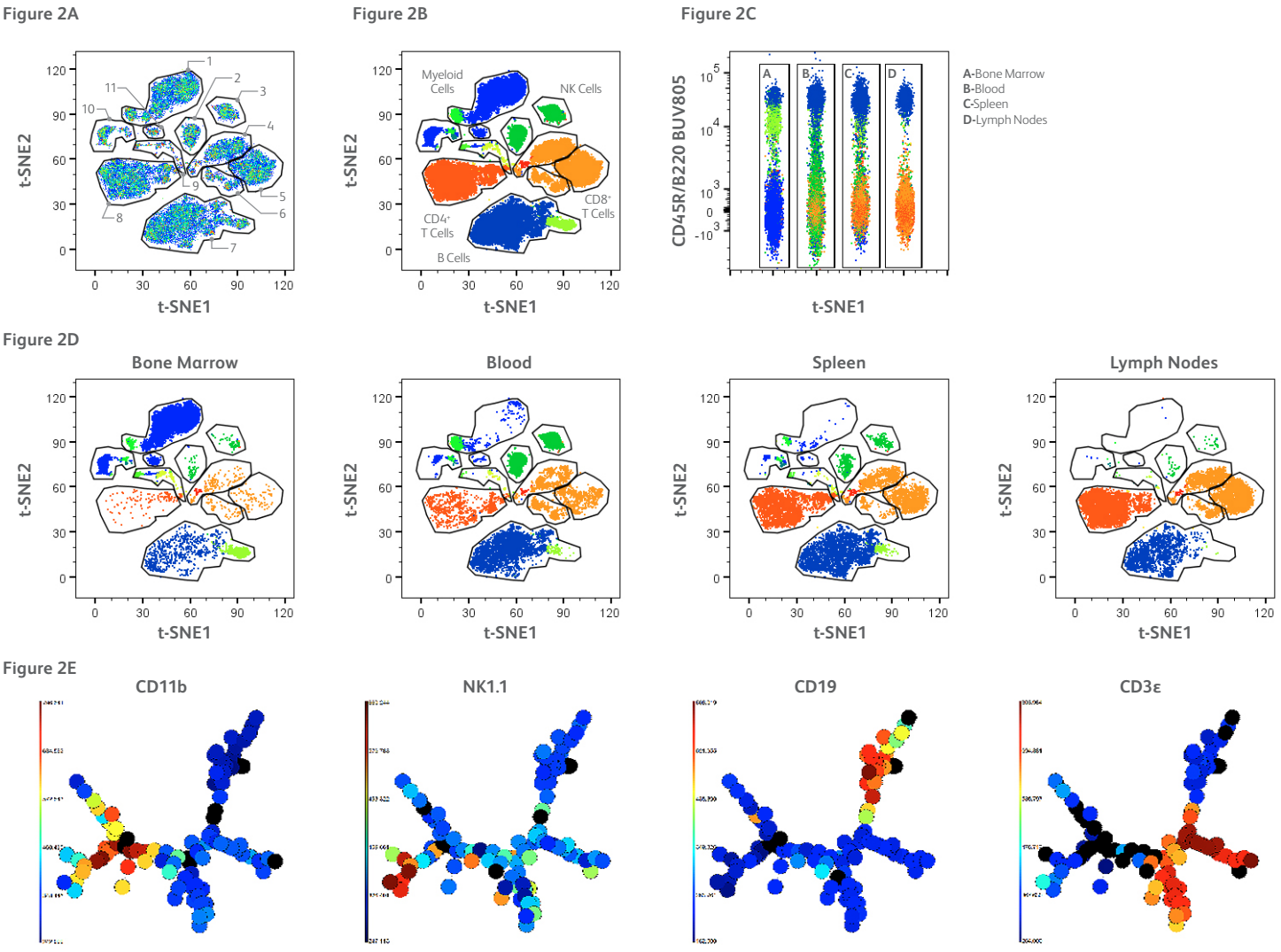

Figure 2. Automated cell clustering analyses showing the distribution of leucocyte populations across mouse tissues

C57BL/6 mouse bone marrow, blood, spleen and lymph node cells were processed following standard protocols for preparation of single cell suspensions. In addition to mechanical tissue dissociation, the splenocytes were also enzymatically digested with Spleen Dissociation Medium from STEMCELL Technologies. After red blood cell lysis with BD Pharm Lyse™ Lysing Buffer, the cells were resuspended in BD Pharmingen™ Stain Buffer (FBS) containing BD Pharmingen™ Purified Rat Anti-Mouse CD16/CD32 (Mouse BD Fc Block™). The cells were subsequently incubated on ice, protected from light, for 30 minutes with a cocktail containing BD Horizon™ Brilliant Stain Buffer Plus and the 27 antibodies listed in Figure 1B. BD Pharmingen™ 7-AAD was added to the samples immediately before cell acquisition on the BD FACSymphony system. **A.** During cell analysis in FlowJo software, doublets and dead cells (7-AAD-positive cells) were excluded and t-SNE analysis was performed after pooling 10,000 singlets/live cells from each tissue. The clusters were arbitrarily enumerated based on relative cell density. **B.** The colored cell clusters corresponding to clusters generated with FlowSOM software were applied onto the t-SNE map. **C and D.** Individual tissue samples were separated using keywords and visualized in the t-SNE map generated from the merged dataset. **E.** The FlowSOM spanning trees represent the expression of key lineage markers. The heatmaps associated with the trees show the expression levels of the indicated markers in the respective tissues. FlowJo v10 software runs FlowSOM using a plugin mechanism.[1]

Dimensionality reduction with t-SNE and clustering analysis with FlowSOM thus enabled a broad comparison of the cell phenotypes derived from blood and lymphoid tissues. Bivariate plots were also employed to assess the staining quality of each marker (Figures 3 and 4). This analysis also allowed the determination of whether t-SNE and FlowSOM could segregate all the predicted leucocyte subpopulations (Figure 5). The gating strategies illustrated in Figures 3 and 4 were used to identify several immune cell subsets.

Figure 3

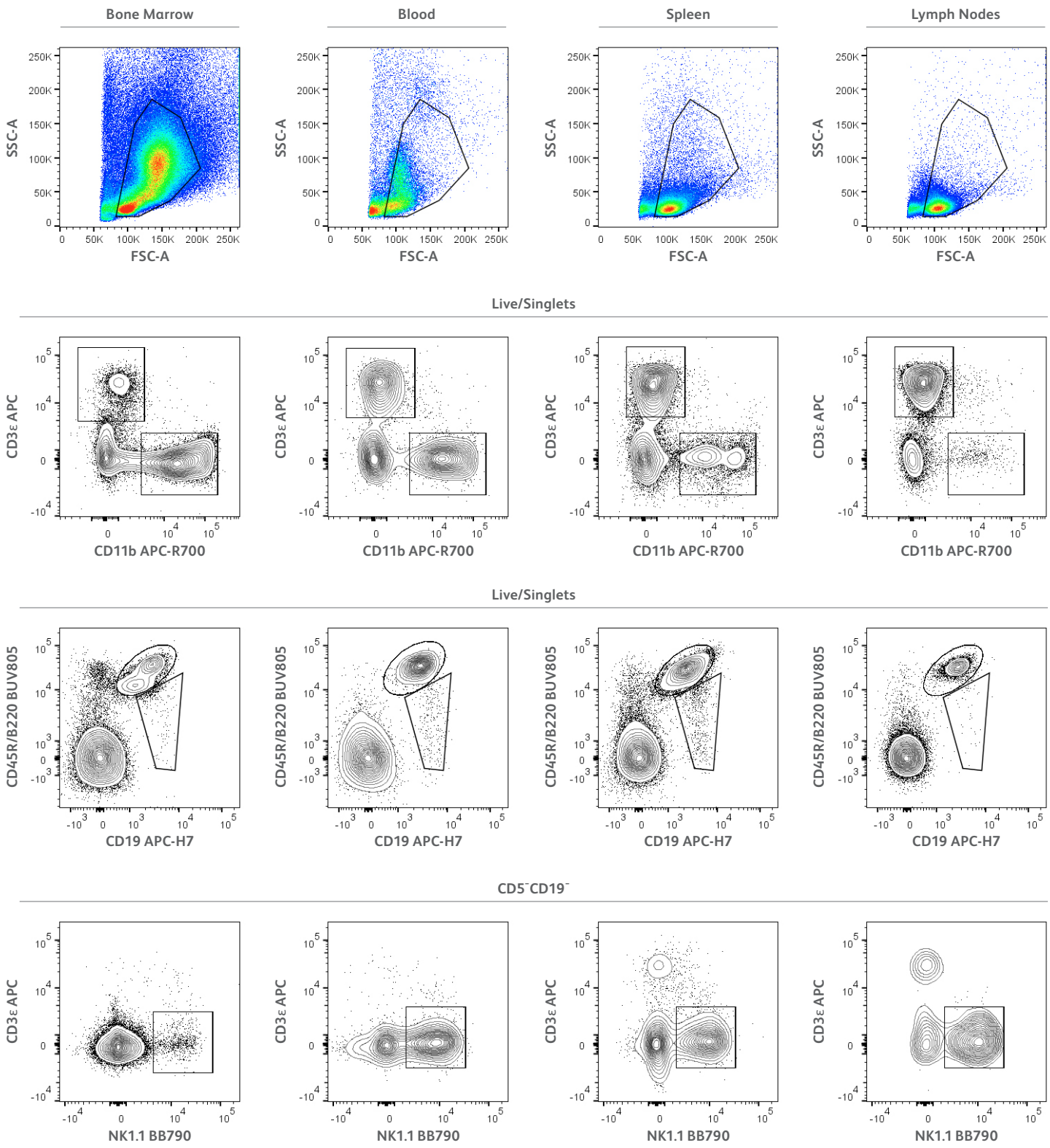

Figure 3. Supervised analysis of leucocyte populations across mouse tissues

The cell samples, stained as described in Figure 2, were analyzed using a traditional manual gating strategy. The major immune cell populations of CD11b$^+$ myeloid cells, CD19$^+$ B cells , CD3ε$^+$ T cells and NK1.1$^+$ NK cells were gated as depicted in the plots. Similar to NK cells, DC populations were also analyzed within the CD5$^-$CD19$^-$ cells (not shown). Sequential gating for further analysis of cell subsets is illustrated in Figure 4.

Among the lymphoid populations, T cells were divided into memory and naïve subsets (Figure 4A), and B cells were scrutinized into the various subsets of immature/transitional and mature cells. Analysis of IgD or CD21 expression in each B-cell subset further confirmed the phenotypes of these populations (Figure 4B). Within NK cells, CD11b^{high}CD27^{low} was the most abundant subset and a fraction of the total NK cells expressed high levels of NKG2A/C/E whereas the expression levels of NKG2D were overall very low (Figure 4C). The myeloid subsets of monocytes, macrophages, DCs and neutrophils were also investigated in the tissues (Figure 4D).

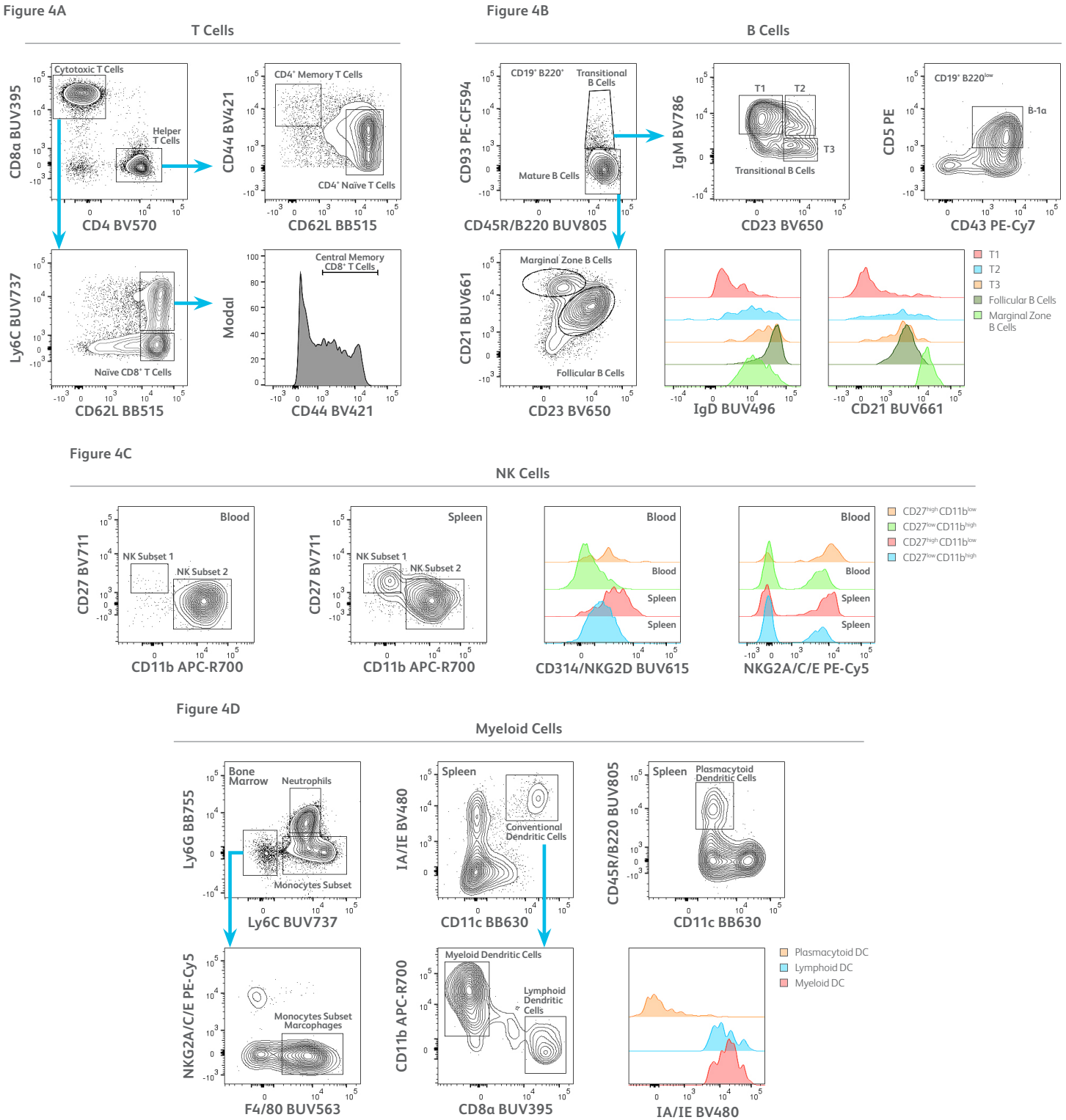

Figure 4. Representative analysis of leucocyte subsets in different mouse tissues

The major immune cell populations of CD11b^{+} myeloid cells, CD19^{+} B cells, CD3^{+} T cells, NK1.1^{+} NK cells and DCs were initially obtained as described in Figure 3. Then, further manual gating was used to define the indicated cell subsets in all four tissues: bone marrow, blood, spleen and lymph nodes. **A.** T-cell subsets in lymph nodes. **B.** B-cell subsets in spleen. **C.** NK-cell subsets in blood and spleen. **D.** Myeloid cell subsets in bone marrow and spleen. The plasmacytoid DC subset was analyzed within the gate of CD5^{-}CD19^{-} CD11c^{+} cells.

When the manually gated populations were overlaid onto the t-SNE map previously created from the merged tissues, each of the gated populations occupied distinct regions in the t-SNE map (Figure 5A). This further demonstrated that t-SNE efficiently segregated the major leucocyte populations and allowed a detailed snapshot of the cell populations in each individual tissue (Figure 5B). Importantly, the cell population overlay did not account for all of the cells in the t-SNE analysis, as clusters of ungated cells were observed in the plot, for example, in cluster six. Further analyses indicated that the cells in this cluster were mostly CD8$^+$ effector memory T cells (data not shown).

Figure 5A

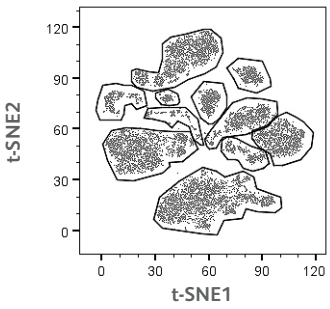

Figure 5B

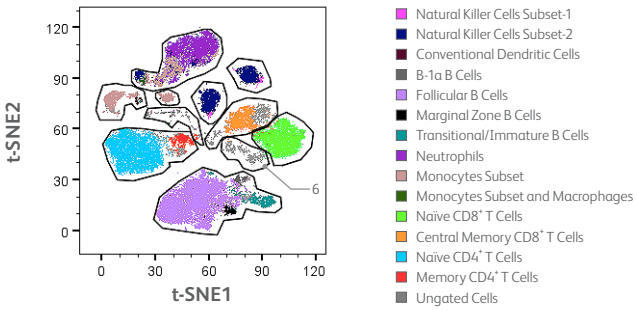

Figure 5C

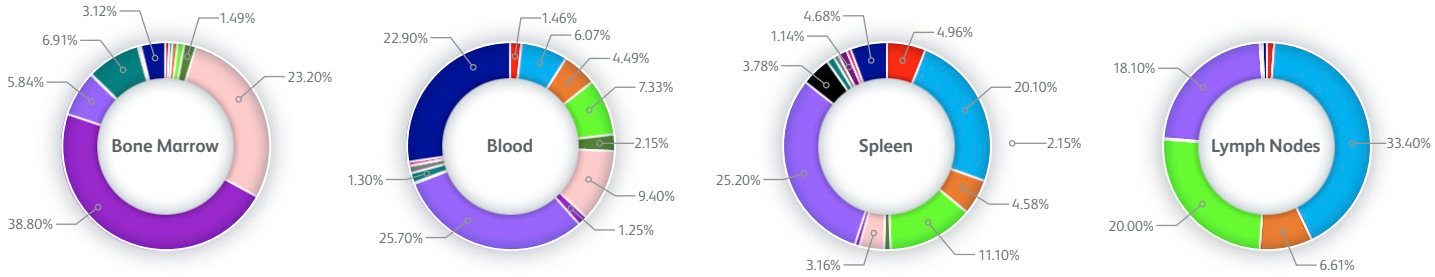

Figure 5. Comparable segregation of cell populations with t-SNE or manual gating strategies

A. Two-dimensional t-SNE map generated after merging cells from bone marrow, blood, spleen and lymph nodes, as described in Figure 2. **B.** The plot depicts a landscape of various cell populations that were manually gated as described in Figures 3 and 4 and overlaid onto the t-SNE plot. **C.** Doughnut charts displaying the frequency of the indicated cell populations in each individual tissue. Cell frequencies higher than 1% are annotated in the graphs.

In conclusion, our results demonstrated that a 28-color panel run on a 30-parameter BD FACSymphony cell analyzer comprehensively probed the phenotypic profiles of various mouse leucocyte populations and subpopulations. The application of dimensionality reduction and clustering algorithms available in FlowJo software enabled clear visualization and automated identification of the cell populations across multiple tissues. Importantly, unsupervised clustering, while recognizing the predicted cell populations, also identified cell subsets missed during supervised analyses of the dataset. This comprehensive single cell profiling application is capable of identifying well-characterized leucocyte populations and has the potential to discover unique cell phenotypes.

References

1. Van Gassen S., et. al. FlowSOM: Using self-organizing maps for visualization and interpretation of cytometry data. Cytometry A. 2015;87(7):636-45.

Ordering information

Reagents	
Description	Cat. No.
BD Pharmingen™ APC-H7 Rat Anti-Mouse CD19	560143
BD Pharmingen™ APC Hamster Anti-Mouse CD3ε	553066
BD Pharmingen™ PE Rat Anti-Mouse CD5	553022
BD Horizon™ APC-R700 Rat Anti-CD11b	564985
BD Horizon™ PE-CF594 Rat Anti-Mouse CD93 (Early B Lineage)	563805
BD Pharmingen™ PE-Cy™7 Rat Anti-Mouse CD43	562866
BD Horizon™ BB515 Rat Anti-Mouse CD62L	565261
BD Horizon™ BV480 Rat Anti-Mouse I-A/I-E	566086
BD Horizon™ BV421 Rat Anti-Mouse CD44	563970
BD Horizon™ BUV395 Rat Anti-Mouse CD8a	563786
BD Horizon™ BV786 Rat Anti-Mouse IgM	564028
BD OptiBuild™ BV711 Hamster Anti-Mouse CD27	740699
BD OptiBuild™ BV650 Rat Anti-Mouse CD23	740456
BD OptiBuild™ BV605 Rat Anti-Mouse CD192 (CCR2)	747969
BD OptiBuild™ BUV805 Rat Anti-Mouse CD45R/B220	748867
BD OptiBuild™ BUV563 Rat Anti-Mouse F4/80	749284
BUV737 Rat Anti-Mouse Ly6C	Custom
BUV661 Rat Anti-Mouse CD21	Custom
BUV615 Rat Anti-Mouse CD314 (NKG2D)	Custom
BUV496 Rat Anti-Mouse IgD	Custom
BV750 Rat Anti-Mouse CD25	Custom
BV570 Rat Anti-Mouse CD4	Custom
BB790 Mouse Anti-Mouse NK1.1	Custom
BB755 Rat Anti-Mouse Ly6G	Custom
BB660 Rat-Anti-Mouse CD127	Custom
BB630 Hamster Anti-Mouse CD11c	Custom
PE-Cy5 Rat Anti-Mouse NKG2A/C/E	Custom
BD Pharmingen™ 7-AAD	559925
BD Pharmingen™ Stain Buffer (FBS)	554656
BD Pharm Lyse™ Lysing Buffer	555899
BD Pharmingen™ Purified Rat Anti-Mouse CD16/CD32 (Mouse BD Fc Block™)	553142
BD Horizon™ Brilliant Stain Buffer Plus	566385

Class 1 Laser Product.

For Research Use Only. Not for use in diagnostic or therapeutic procedures.

23-21380-00

BD Life Sciences, San Jose, CA, 95131, USA

bdbiosciences.com